

Cationic Peptides Facilitate Iron-induced Mutagenesis in Bacteria

Alexandro Rodríguez-Rojas*, Olga Makarova, Uta Müller and Jens Rolff *

Evolutionary Biology, Institute for Biology, Free University Berlin, Berlin, Germany.

*Corresponding authors: a.rojas@fu-berlin.de, jens.rolff@fu-berlin.de. Königin-Luise-Strasse 1-3, 14195 Berlin, Germany.

Short title: Cationic peptides and iron mutagenesis in bacteria

1 Abstract

2 *Pseudomonas aeruginosa* is the causative agent of chronic respiratory infections and is
3 an important pathogen of cystic fibrosis patients. Adaptive mutations play an essential
4 role for antimicrobial resistance and persistence. The factors that contribute to
5 bacterial mutagenesis in this environment are not clear. Recently it has been proposed
6 that cationic antimicrobial peptides such as LL-37 could act as a mutagen in *P.*
7 *aeruginosa*. Here we provide experimental evidence that mutagenesis is the product of
8 a joint action of LL-37 and free iron. By estimating mutation rate, mutant frequencies
9 and assessing mutational spectra in *P. aeruginosa* treated either with LL-37, iron or a
10 combination of both we demonstrate that mutation rate and mutant frequency were
11 increased only when free iron and LL-37 were present simultaneously. The addition of
12 an iron chelator completely abolished this mutagenic effect, suggesting that LL-37
13 enables iron to enter the cells resulting in DNA damage by Fenton reactions. This was
14 also supported by the observation that the mutational spectrum of the bacteria under
15 LL-37-iron regime showed one of the characteristic Fenton reaction fingerprints: C to T
16 transitions. Free iron concentration in nature and within hosts is kept at a very low
17 level, but the situation in infected lungs of cystic fibrosis patients is different.
18 Intermittent bleeding and damage to the epithelial cells in lungs may contribute to the
19 release of free iron that in turn leads to generation of reactive oxygen species and
20 deterioration of the respiratory tract, making it more susceptible to the infection.

21

22

23

1 **Author Summary**

2 Cationic antimicrobial peptides (cAMPs) are small proteins naturally produced by the
3 immune system to limit bacterial growth mainly through pore formation in the
4 membrane. It has recently been suggested that sub-inhibitory concentrations of
5 cAMPs promote bacterial mutagenesis, similarly to antibiotics. However, we previously
6 reported that cAMPs do not increase mutation rate and do not activate bacterial stress
7 responses. Here we resolve this contradiction. We report that free iron in the culture
8 medium increases mutagenesis in the presence of cAMPs. We show that sub-inhibitory
9 concentrations of cAMPs facilitate entry of free iron into bacterial cells, where it
10 interacts with hydrogen peroxide, thereby resulting in production of DNA-damaging
11 reactive oxygen species and increased mutagenesis. Moreover, these results may have
12 clinically-relevant implications: while very little free iron is normally present in healthy
13 individuals, this is not the case in patients suffering from cystic fibrosis, where elevated
14 bacterial mutagenesis promotes antibiotic resistance and contributes to persistence
15 and severity of infection. Thus, an intervention aimed at reduction of free iron in the
16 lungs could reduce the cAMPs-facilitation of iron-mediated mutagenesis; hence
17 antibiotic resistance and pathoadaptation.

18

19

20

21

22

1 Introduction

2 *Pseudomonas aeruginosa* is an important opportunistic pathogen involved in chronic
3 respiratory and hospital-acquired infections [1]. In cystic fibrosis (CF) patients, one of
4 the most common genetic diseases in humans, this bacterium causes chronic lung
5 infections that result in significant morbidity and mortality [2]. *P. aeruginosa* infections
6 are difficult to treat due the inherent resistance to many drug classes, its ability to
7 acquire resistance, via mutations, to all relevant treatments and its high and increasing
8 rates of resistance locally [3].

9 Mutagenesis plays a crucial role in adaptation of this pathogen for persistence and
10 antibiotic resistance acquisition in CF [4], being found a high proportion of
11 hypermutable bacteria among *P. aeruginosa* isolates [5]. Recently, Limoli *et al* [6]
12 reported an increased mutant frequency after treatment of *P. aeruginosa* with the
13 human cationic peptide LL-37. Based on this finding they proposed that cationic
14 peptides elevated bacterial mutation rates. In a recent study, we reported mutation
15 rates of *E. coli* in the presence of cationic antimicrobial peptides (cAMPs) and
16 antibiotics. LL-37 was present in the panel of AMPs that we tested and we did not find
17 any increase in mutation rates. We also used transcription reporter assays and qRT-
18 PCR and showed that none of the AMPs elicited the main mutagenic stress pathways
19 of bacteria SOS or *rpoS* [7].

20 Here, we aim to resolve this apparent contradiction based on the observation that the
21 different studies used different media. Limoli *et al.* [6] used M63 for *P. aeruginosa* and
22 LB for *E. coli*, while we used non-cation adjusted Mueller-Hinton Broth (MHB),
23 commonly used for cAMP susceptibility testing . The most striking difference in culture

media between the two studies is that both, M63 [8] and LB are iron-rich [9,10], while MHB is not [11]. Fe^{2+} catalyses hydroxyl radical formation by reacting with hydrogen peroxide both intra- and extra-cellularly, the Fenton reaction [12]. Without free iron hydrogen peroxide reactivity is low at physiological pH and iron metabolism is strictly controlled to avoid DNA and other damage caused by oxygen radicals [13,14]. In most natural situations iron is in short supply, but in cystic fibrosis [15,16] due to accult bleeding of highly vascularised lung tissue and haemoptysis particularly during acute exacerbations, and damage of the respiratory tract epithelium where Fe^{2+} is present intermittently. Although ferrous iron is prone to oxidation, the anaerobic growth of at to high density of bacteria [17] may contribute to stabilise this metal in the reduced state.

Many cationic antimicrobial peptides change membrane permeability properties [18], and this led us to hypothesize that sub-inhibitory concentrations of LL-37 increase uncontrolled iron transport from the extracellular space to the cytoplasm without the intervention of the bacterial iron trafficking system. An intracellular surplus of iron should then result in DNA damage caused by the Fenton reaction.

Here, we (i) estimate the mutation rate of *P. aeruginosa* in the presence of LL-37, iron or both; (ii) we then investigate the hypothesis that ferrous iron (Fe^{+2}) is causal to an increase in mutation rate and that LL-37 facilitates this process, something that is true for colistin too; and finally (iii) we investigate the mutational spectra to find out if promoted mutations match with any of the molecular signatures of Fenton reactions.

22

23

1 Results and Discussion

2 Mutation rate is increased in the presence of ferrous Fe^{2+} and LL-37

3 First we determined the mutation rate of *P. aeruginosa* using a fluctuation assay, in
 4 the presence of either LL-37 (32 $\mu\text{g/ml}$), Fe^{2+} (40 μM), or both (figure 1). Mutation rate
 5 was only increased when LL-37 and Fe^{2+} were added simultaneously, while addition of
 6 LL-37 or Fe^{2+} separately did not produce the same effect. To investigate the effect of
 7 different concentrations of LL-37 and Fe^{2+} , we estimated mutant frequencies. None of
 8 the LL-37 concentrations tested, ranging from 4 to 32 $\mu\text{g/ml}$, yielded any detectable
 9 changes in mutant frequency (figure S1). Fe^{2+} alone, at different concentrations, also
 10 did not increase the mutant frequencies in comparison with the control group (figure
 11 S2).

12
 13 **Figure 1. The joint action of LL-37 and ferrous ions induces an increase in the**
 14 **mutation rate of *P. aeruginosa*.** No changes occur when LL-37 or iron are added to the
 15 culture separately. Error bars represent 95 % confidence intervals for mutation rates.

16 Subsequently, we assayed the MIC50 (32 $\mu\text{g/ml}$) of LL-37 with several iron
 17 concentrations and measured the impact on rifampicin mutant frequency of *P.*
 18 *aeruginosa* strain PAO1. We found that added concentrations of 10, 20, 40 and 80 μM
 19 of Fe^{2+} , increased the mutant frequency between three to five times (figure S3).

20 Limoli *et al.* [6] observed increased mutant frequencies in both, *P. aeruginosa* and *E.*
 21 *coli*, proposing that LL-37 induces mutagenesis in these bacteria. Taken at face value,
 22 this contrasts with our work, where we did not find such effect in *E. coli* [7]. *P.*
 23 *aeruginosa* in the Limoli *et al.* study however, was cultured in an iron-rich medium,

1 M63 [8], which contains 0.5 mg of iron sulphate per litre (Fe^{2+}). To confirm the results
 2 in a different bacterial model, the experiment was repeated with *E. coli* using LB as a
 3 culture medium. However, LB is also iron-rich (~16 μM of iron) [9,10]. In these
 4 experiments, just before the treatment with LL-37 in a saline solution, bacteria were
 5 washed. It has, however, been shown that Gram-negative bacteria can actively
 6 accumulate iron in the periplasmic space [19]. This led us to hypothesise that sub-
 7 lethal concentrations of cationic antimicrobial peptides can facilitate iron transport
 8 into the cells.

10 **LL-37 facilitates mutagenesis but iron is causal**

11 To confirm that iron is causing the observed increase in mutagenesis, we first repeated
 12 the assay in the presence of an iron chelator, 2-2' bipyridyl. 2-2' bipyridyl completely
 13 abolished the increase in mutant frequency in the tested concentration of LL-37+ Fe^{2+}
 14 combination. The sole action of the chelator plus Fe^{2+} did not increase the mutant
 15 frequency (figure 2).

17 **Figure 2. The mutagenesis of LL-37+ Fe^{2+} combination is suppressed by the addition of**
 18 **an iron chelator.** This supports the notion that iron is causal in increasing mutagenesis
 19 (A). In the same line, over-expression of Dps, a natural iron chelator in bacteria, also
 20 decreases the mutant frequency to rifampicin (B). Error bars represent 95 %
 21 confidence intervals for mutant frequencies.

22 Bacteria have a number of mechanisms to keep free iron as low as possible inside the
 23 cell. One of these is Dps, a natural iron chelating protein. To confirm the results
 24 obtained with 2-2' bipyridyl, we used a Dps over-expressing strain by cloning the *dps*

1 gene into a multi-copy plasmid under a constitutive promoter. The mutagenesis was
2 not completely reverted in comparison with non-treated controls, but there was a 1.8
3 fold-reduction (figure 2).

4 The iron uptake assay showed that there was a significant difference ($P=0.00015$) in
5 total iron content in bacterial cells between LL-37+ Fe^{2+} (17.50 ± 5.10 nmoles/ml, mean
6 \pm standard deviation) and iron alone (5.65 ± 4.13 nmoles/ml, mean \pm standard
7 deviation) treatments after 30 minutes of incubation, indicating that LL-37 indeed
8 promotes a non-physiological free iron entrance.

9 We also tested a further AMP: Colistin, which is of bacterial origin, and is one of the
10 most effective agents against *P. aeruginosa* in CF infections [20]. We treated cultures
11 of *P. aeruginosa* PAO1 with MIC50 of colistin ($1.8 \mu\text{g/ml}$) in high and low
12 concentrations of iron in the media. The effects of colistin were very similar to the
13 effects we found for LL-37 (figure 3). Although the mechanism of action of colistin is
14 not fully understood [21], our results suggest pore forming mechanism or permeability
15 changes in the cell as likely mechanisms. It has been demonstrated that colistin
16 promotes the uptake of hydrophilic antibiotics, explaining their synergism with them
17 [22].

18 **Figure 3. Mutagenesis induced by colistin and Fe^{2+} combination.** The mutation rate is
19 only increased if both, iron and colistin, are present. Error bars represent 95 %
20 confidence intervals for mutation rates.

21 Previous work has suggested that iron is involved in *Pseudomonas aeruginosa*
22 pathoadaptation and antibiotic resistance acquisition [15]. All experiments were
23 carried out with the more soluble Fe^{2+} because ferrous iron is abundant in the CF lung

1 (~39 μ M on average for severely ill patients) and significantly correlates with disease
 2 severity [23]. Moreover, iron activates the two-component signal transduction system
 3 BqsRS in *P. aeruginosa*, which is transcriptionally active in CF sputum, and promotes
 4 tolerance to cationic stressors [24]. This increases the tolerance to both host peptides
 5 such as LL-37 and colistine, which is administered in CF therapy.

6 The new mechanism proposed here has almost certainly important implications. Under
 7 specific pathologies such as cystic fibrosis or other respiratory chronic diseases, iron
 8 that is usually in short supply, is abundant. Disturbances in iron metabolism have been
 9 shown to promote evolution of antibiotic resistance in *E. coli* [25]. Given that cationic
 10 antimicrobial peptides usually induce membrane permeability in all susceptible
 11 microbes and Fenton chemistry is universal, the mechanism we propose here is likely
 12 applicable to other AMPs. For example, beta-defensin-2 was shown to double the
 13 mucoid conversion rate, a mutagenic process, of *P. aeruginosa* [6]. Yet free iron is
 14 rarely available in most physiological situations but for a few pathologies such as cystic
 15 fibrosis

16 Additionally, it has been reported that some cationic antimicrobial peptides interact
 17 with bacterial membrane proteins and delocalise them [26]. It is conceivable then that
 18 LL-37 may interact and interfere with iron transport systems, which in turn may
 19 contribute to iron homeostasis disruption and enhance mutagenesis. This possibility
 20 requires additional investigation and will be the goal for future studies.

21 In the context of cystic fibrosis, the increase in salt concentration may lead to the
 22 reduced activity or complete inactivation of other antimicrobial peptides, as observed
 23 for human beta-defensin-1 [27], while other components could eventually contribute
 24 to mutagenesis in the same way that LL-37 does. Moreover, the PhoP-PhoQ and PmrA-

1 PmrB two-component regulatory systems of *P. aeruginosa* may play an important role
 2 in antimicrobial peptide tolerance. This resistance is reproduced *in vitro* when
 3 magnesium concentrations are low [28]. Our experimental conditions, where divalent
 4 cations are depleted or in low concentrations, seem comparable. In the light of our
 5 results this suggest that bacteria under certain conditions that elicit the expression of
 6 these two component systems alter the lipidA structure resulting in increased
 7 resistance to colistin [29]. The same systems up-regulate ferrous iron uptake which is
 8 mediated by feoAB operon [28,30]. This phenomenon could potentially contribute to
 9 saturate intracellular iron storage systems and to generate an excess of iron that
 10 eventually can participate in Fenton reaction operating by the mechanisms that we
 11 propose here.

12 How would the mechanism we propose here enhance the overall mutation rate of
 13 bacterial populations? In the context of cystic fibrosis, there is a high proportion of
 14 hypermutable bacteria due to the inactivation of their DNA miss-match repair (MMR)
 15 genes [31]. We may expect a synergistic effect of both types of mutagenesis as we
 16 proposed in the past for the mutagenic effect of cystic fibrosis lung environment and
 17 the intrinsic mutagenesis of *P. aeruginosa* [4]. It can be speculated that iron-
 18 mutagenesis can facilitate the rise of mutator bacteria by enhancing the inactivation of
 19 MMR genes. This could then weaken genetic constraints that impede the evolution of
 20 bacteria to resist antibiotics by multiple pathways as previously described [32].

21 **Mutational spectra of iron-induced mutagenesis.**

22 The results above strongly suggest that sub-lethal concentrations of cationic
 23 antimicrobial peptides facilitate the access of free iron to the cytoplasmic

1 compartment of *P. aeruginosa*. Given that the Fenton reaction results in DNA damage
2 [33] and reactive oxygen species (ROS) damages to the DNA display specific molecular
3 fingerprints, we investigated if there was evidence of the Fenton reaction effects on
4 the mutational spectrum.

5 It would be very difficult to investigate the mutational spectrum in *rpoB* (sub-unit of
6 RNA polymerase) that confers resistance to rifampicin in *P. aeruginosa* PAO1. This
7 gene is essential in and detectable mutations are mostly point mutations that would
8 constrain the analysis to a few types of changes. We therefore decided to use another
9 strain, PA14, where mutations that confer resistance to fosfomycin are well
10 characterized [34–36]. Resistance mutations to fosfomycin in *P. aeruginosa* PA14
11 depend on a single non-essential locus encoding the glycerol-3-phosphate transporter
12 GlpT, making it a much better marker for studying the entire repertoire of mutations
13 compared to *rpoB* [36,37] [38].

14 The treatment of *P. aeruginosa* P14, which shows a similar sensitivity to LL-37 as the
15 PAO1 strain used above, with the mutagenic combination of LL-37+Fe²⁺ showed almost
16 a four fold-increase in mutant frequency (figure S4).

17 To assess how addition of free iron and antimicrobial peptides affect the mutation
18 spectrum of the *glpT* gene of PA14 strain we exposed bacteria to either free iron,
19 antimicrobial peptide LL-37, or both. All of the resulting resistant mutants contained
20 non-synonymous substitutions or deletions in *glpT* that potentially affect the stability
21 of GlpT transporter and likely disrupt the function of the protein (figure 4, table S1,
22 figures S5 and S6). LL-37+Fe²⁺-treated bacteria displayed striking differences in
23 mutational spectra when compared to the other treatments (figure 4 and table S1).

1 We used Monte Carlo hypergeometric test implemented in iMARS, a mutation analysis
2 reporting software [39], to assess the overall differences between mutational spectra.
3 The probability of the mutational spectra to be the same stood at 0.554706 (P -value
4 confidence limits 0.531080 – 0.578) when the iron treatment was compared to LL-37,
5 but was below 0.0000001 when either were compared with LL-37+Fe²⁺ treatment.
6 Moreover, we found a mutation hotspot (R93 to W change, 10/20 clones) in the LL-
7 37+Fe²⁺ treatment group that was significantly ($P=0.0004$, two-tailed Fisher's exact-
8 test) different from the two other treatments (tables S2, S3 and S4). This mutation
9 hotspot is a single nucleotide transition from C to T, which is one of the most frequent
10 types of mutations caused by ROS [40]. We found that twelve out of twenty clones
11 from the LL-37+Fe²⁺ condition had C to T transitions, whereas none were present in
12 either iron or LL-37- treated bacteria (two-tailed Fisher's exact-test ($P<0.0001$) (figure
13 S7). It is striking that although several C to T mutations can potentially lead to *glpT*
14 inactivation are in principle possible, that the majority are concentrated in a single
15 point. Such mutation hotspots can be driven by a specific topology on the
16 chromosome [41], or a particular sequence prone to double strand breaks resulting in
17 mutations after repair [42]. In general, observable mutations are the results of
18 mutation-repair balance and not all mutations are repaired with the same efficiency. A
19 good example in *P. aeruginosa* is the mutational inactivation of the anti-sigma factor
20 gene, *mucA*, with the mutated allele *mucA22* most prevalent (25 to 40%). This
21 inactivation seems to be spectrum dependent [43].

22 **Figure 4. Mutation hotspots in *glpT*.** Distribution of the mutations in the 1160 bp-long
23 fragment of *glpT* in *P. aeruginosa* PA14 fosfomycin-resistant clones treated with iron,
24 LL-37, or a combination of both. The number of mutations (nucleotide substitutions,

1 indels) is plotted against respective nucleotide positions within the gene fragment.
 2 Note the overlapping mutations at positions 220-225, 409 and 524 bp in iron and LL-37
 3 treatments and absence of common mutations in LL-37+Fe²⁺ treatment. The figure was
 4 generated using the mutational spectrum analysis software iMARS [39].

5 Interestingly, C to T transitions were one of the most frequent types of single
 6 nucleotides changes in the genomes of *Salmonella typhimurium* evolved to increasing
 7 concentrations of LL-37 in modified LB medium short of sodium chloride and anions
 8 [44], which is fully consistent with our results.

9 A number of studies [45–48], which caused some controversy [49–51], suggested that
 10 hydroxyl radicals can be generated as a consequence of antibiotic treatments and this
 11 aggressive by-product may take part in the killing mechanism of bactericidal drugs or
 12 promote mutagenesis. Most of these studies were carried out in the iron-rich LB
 13 medium and whether processes as described here for the interaction between an AMP
 14 and iron apply to antibiotics remains to be explored.

15 **Conclusions**

16 Our results support the notion that under certain pathological situations, sub-
 17 inhibitory concentrations of cAMPs facilitate uncontrolled uptake of free iron by
 18 bacterial cells, which results in increased mutagenesis by Fenton reaction (figure 5).
 19 According to our results, this could be a general mechanism underlying mutagenesis by
 20 joint action of antimicrobial peptides and free iron in specific situations where iron is
 21 not limited.

1 **Figure 5. A model for LL-37-mediated, iron-induced mutagenesis in *Pseudomonas***
2 ***aeruginosa*.** The interactions of LL-37 with the membrane at sub-inhibitory
3 concentrations lead to transient permeability changes in the membranes that promote
4 iron movement in favour of the electrochemical gradient. Uncontrolled uptake of
5 ferrous ions stimulates Fenton reaction that leads to hydroxyl radical formation and
6 results in DNA damage and mutagenesis.

7 Free iron levels are kept as low as possible due to its toxic effect for all living beings but
8 especially in bacteria that lack proper cell compartments. In fact, iron withdrawal is
9 part of the natural innate immune response in inflammation that makes free iron even
10 more scarce. During inflammation and infection a “hypoferremic response” (anaemia
11 of inflammation) is observed [52,53]. Many chelating proteins such as transferrin and
12 ferritin exhibit antibacterial activity simply by making iron availability incompatible
13 with bacterial proliferation [54].

14 Despite showing that many cationic antimicrobial peptides are unable to increase
15 mutation rates [7], the particular situation of iron-induced mutagenesis can be of great
16 interest for certain types of infections where iron homeostasis is compromised. In
17 cystic fibrosis, bleeding happens frequently. Considering that *P. aeruginosa* is one of
18 the most common pathogens that acquire all antibiotic resistance by mutations, the
19 mechanism proposed here is likely very relevant for pathoadaptation.

20 Finally, our work has potential implications for the development of future treatment of
21 chronic respiratory infections by *Pseudomonas aeruginosa*. For example, modulation
22 of iron-chelating agent in CF therapy could potentially slow down the pathoadaptation
23 and development of resistance in CF, and diminish lung damaging by ROS.

1 **Materials and methods**

2 **Bacteria and growth conditions.** The *P. aeruginosa* PAO1 wild-type strain was kindly
 3 provided by M. A. Jacobs. The *P. aeruginosa* PA14 was kindly provided by Nicole T.
 4 Liberati and Frederick Ausubel. All bacterial strains were cultured in Mueller-Hinton
 5 Broth, non-cation adjusted (Sigma), with total iron content $0.22 \pm 0.02 \mu\text{M}$, following
 6 recommendations of CLSI for cationic antimicrobial peptide susceptibility testing. The
 7 MHB pH was adjusted to 6 in all cases with acetic acid to enhance solubility of both, LL-
 8 37 and iron compound. All experiments were performed at 37°C , under agitation in
 9 liquid culture. For genetic manipulation, *Escherichia coli* DH5 α strain was used and
 10 routinely cultured in Lysogeny Broth (LB medium), supplemented with antibiotic when
 11 appropriate.

12 **Minimal inhibitory concentration (MIC).** MICs were determined according to CLSI
 13 recommendations by a microdilution method with some modifications for
 14 antimicrobial peptides. The MIC was defined as the antimicrobial concentration that
 15 inhibited growth after 24 hours of incubation in liquid MHB medium at 37°C .
 16 Polypropylene non-binding multi-well plates (Th. Geyer, Germany) were used for all
 17 experiments.

18 **Determination of MIC50.** The MIC50s for all antimicrobials were determined by
 19 inoculating strains grown to mid-log phase into the wells of a 96-microwell plate.
 20 Approximately 10^2 cells from overnight cultures of PAO1 and PA14 strains were
 21 inoculated into 50 ml tubes containing 10 ml of MBH and incubated at 37°C with
 22 strong agitation until the mid-log phase of growth (approximately 10^8 cfu/ml). Then,
 23 $100 \mu\text{l}$ of 2×10^8 cells from these cultures were inoculated in each well of

1 polypropylene non-binding 96-multiwell plates containing 100 μ l of fresh Mueller-
 2 Hinton medium with growing concentration of serially diluted LL-37. The plates were
 3 incubated at 37°C during four hours with continuous agitation in a plate reader
 4 (Synergy HT, BioTek). Four replicates per concentration were prepared and the
 5 experiments were repeated twice. MIC50s at 4 hours were defined as the
 6 concentrations at which 50% of growth reduction in comparison to the control at
 7 OD₆₀₀ were observed.

8 **Estimation of mutant frequencies and mutation rates.** For spontaneous-mutation rate
 9 measurements of PAO1 strain, 1/100 dilutions of overnight cultures were inoculated
 10 into four tubes per group, each containing two ml of MHB medium. The cultures were
 11 incubated at 37°C with strong agitation to reach $\sim 10^8$ cfu/ml. At this point, appropriate
 12 concentration of LL-37, colistin, iron sulphate (FeSO₄) or combinations of antimicrobial
 13 peptides and iron, were added to the cultures. The tubes were allowed to continue
 14 their normal growth overnight until saturation. In the experiments with colistin, the
 15 bacterial suspensions were washed twice with saline solution 0.9 % NaCl before
 16 plating. The cultures were appropriately diluted and plated on MHB agar plates with or
 17 without rifampicin (100 μ g/ml). The mutant frequency was estimated by the number
 18 of colonies growing on rifampicin divided by the number of total cfu/ml. To confirm
 19 the results, relevant concentrations were also assayed with ten replicates to see the
 20 influence of the treatment on the population mutation rates (the number of mutations
 21 per cell per generation). Mutation rates were calculated by maximum verisimilitude
 22 method and data were processed using the on-line web-tool Falcor
 23 (<http://www.mitochondria.org/protocols/FALCOR.html>) as recommended [55,56].
 24 Falcor software was used to estimate the mutant frequency too. The mutation rates

for the strain PA14 under the selected treatments were determined in the same way as described for PAO1, but fosfomycin (128 µg/ml) was used instead of rifampicin.

Sequencing of fosfomycin resistant mutants (Fos-R) and sequence analysis. To assess the effects of iron and antimicrobial peptides and their combination on the mutation spectrum of *P. aeruginosa* strain PA14, the *glpT* gene of twenty randomly selected Fos-R clones from independent cultures for each treatment group (MHB supplemented either with 40 µM Fe²⁺, LL-37 (32 µg/ml) or a combination of LL-37+Fe²⁺ at same concentrations for both), was amplified by colony PCR using *glpT*-P14-F1 (5-AGCGGAGCTCGCGATGTTC-3) and *glpT*-P14-R1 (5-TCAGCCGGCTTGCTGCGG-3) primers [36] and Kapa2G Fast ReadyMix PCR with dye kit (KAPA Biosystems, Boston, US). Cycling conditions were as follows: 95°C 7'/(95°C 15''/60°C 15''/72°C 40'')x 35/72°C 7'/4°C hold. The PCR products were purified and sequenced at Macrogen Europe using the forward and reverse primers described above. Sequences were assembled using SeqTrace software. Assembled sequences were imported into CLC Sequence Viewer 6 and aligned using default settings. Low quality flanking sequences were removed and the alignment was trimmed to the 1160 bp fragment (the 52-1212 bp region relative to the A in the start ATG codon of the 1347bp-long *glpT* ORF). A tridimensional homology model of GlpT was generated using Cn3D software by performing a BLASTP search using PA14 strain GlpT protein sequence as a query and mapping the resulting alignment against the experimentally determined *Escherichia coli* K-12 GlpT protein structure. To evaluate the potential effects of amino acid substitution on protein stability, the online tool I-Mutant (<http://gpcr2.biocomp.unibo.it/cgi/predictors/I-Mutant3.0/I-Mutant3.0.cgi>) was used. TMHMM server v. 2.0 (<http://www.cbs.dtu.dk/services/TMHMM/>) was used for prediction of

transmembrane helices in *glpT* protein sequence. Mutational spectrum differences were analysed using the software iMARS [39].

Influence of 2-2' bipyridyl on LL-37+Fe²⁺ mutagenesis. The effect of 2-2' bipyridyl, an iron chelating agent, on LL-37+Fe²⁺ mutagenesis was determined by measuring its influence on mutant frequency on a selected concentration of LL-37+Fe²⁺ combination (32 µg/ml and 40 µM of Fe²⁺ respectively), where mutagenesis was observed. The experiment consisted of adding a titrating concentration of 2-2' bipyridyl (114 µM) to chelate 95 % of the added iron of treated cultures, in order to make the treatment compatible with bacterial growth. Cultures with the described LL-37+Fe²⁺ combination with no addition of 2-2' bipyridyl were used as a control. The mutant frequencies of both groups were determined as described elsewhere in this section. LL-37, iron and 2-2' bipyridyl were simultaneously added to the exponentially growing cultures.

Cloning of *dps* gene and mutagenesis experiment. DNA fragment containing the PAO1 *dps* gen from genomic DNAs was amplified by PCR using the oligonucleotides PA-DPS-F1 (5'-ATGGAAATCAATATCGGAATCG-3') and PA-DPS-R1 (5'-CTACTCAAATCAAGCGTTGGC-3') as forward and reverse primers, respectively. The fragment contains the ATG codon and 50 nucleotides downstream of the stop codon. The PCR product was directly cloned into the *Sma*I-digested and T-tailed pUCP24 plasmid vector (replicative in both *P. aeruginosa* and *E. coli*), which harbours Gentamicin resistance markers [57]. *E. coli* DH5α was used following standard protocols for genetic manipulations. The resulting plasmids, termed pUCP24-DPS, were introduced by electroporation into PAO1 wild type strain. The cloning vector was also transformed into the same strain as control. An experiment similar to the one designed for 2-2' bipyridyl was carried out. A mutagenic combination of LL-37+Fe²⁺ was

1 assayed in the strains carrying pUCP24-DPS plasmid or the empty vector pUCP24 and
2 mutant frequencies were determined for both groups.

3 **Quantification of iron concentrations.** Total iron quantification was carried out as
4 previously described with minor modifications [58,59]. Cultures of *P. aeruginosa* PAO1
5 were grown to an OD₆₀₀ of approximately 0.5 at 37°C with agitation in a volume of two
6 ml in MHB. The cultures were centrifuged at 4000 *g* during ten minutes at 20°C. The
7 pellets were re-suspended in fresh MHB and three different groups were prepared.
8 The treatments consisted of LL-37 (32 µg/ml) (I), iron sulphate to a final concentration
9 of 40 µM (II), a combination iron sulphate and LL-37 (III), both of them at the same
10 concentrations of their respective group I and II, and a control group (IV) to which the
11 proportional amounts of LL-37 and iron sulphate solvent were added (sterile dH₂O and
12 dH₂O, pH=5 respectively). The cultures were incubated for up to 30 minutes and
13 harvested by centrifugation as before but at 4°C. The cell pellets were washed twice
14 with ice-cold phosphate-buffered saline (PBS) and re-suspended in 1 ml of TE buffer
15 containing 5 mg/ml of egg lysozyme (Sigma) and incubated during 10 minutes at room
16 temperature. To quantify total iron, the lysate (one ml) was mixed with one ml of HCl
17 10 mM and 1 ml of iron-releasing reagent containing HCl 1.4 M + 4.5%
18 (weight/volume) aqueous solution of KMnO₄; 1/1 and incubated at 60°C for two hours.
19 After cooling, 0.06 ml iron-detection reagent (6.5 mM ferrozine, 6.5 mM neocuproine,
20 2.5 M ammonium acetate, 1 M ascorbic acid in water) was added and the sample
21 absorbance was read at 550 nm in a plate reader Synergy HT (Biotek). The iron
22 concentrations were determined based on a standard curve obtained with increasing
23 concentrations of ferric chloride and normalized to protein concentration of the
24 lysates. Each group consisted of five cultures. We determined the content of total iron

1 in our cultures media MHB and LB, using the same procedure describe above, starting
2 by the addition of 1 ml of HCl 10 mM and 1 ml of the iron-releasing reagent. Under the
3 suspicion that MHB had lower iron content, the samples of this medium were
4 prepared ten-fold concentrated.

5 **Statistical analyses.** An unpaired Student's t test or Mann-Whitney U test was used
6 where appropriate for statistical analysis, according to the nature of the data
7 (parametric or nonparametric adjustment). Two-tailed Fisher's exact test or Monte
8 Carlo hypergeometric test were used to calculate statistical significance of differences
9 in mutation frequencies at each codon site of the alignment between treatments in
10 the mutational spectrum analysis. P values less than 0.05 were considered statistically
11 significant. All tests were performed with statistic software R except for mutational
12 spectrum analysis where iMARS [39] was used instead.

13

14 **Acknowledgments.** We are grateful to Paul Johnston for comments on the manuscript.

15 **References**

- 16 1. Stover CK, Pham XQ, Erwin AL, Mizoguchi SD, Warrenner P, Hickey MJ, et al.
17 Complete genome sequence of *Pseudomonas aeruginosa* PA01, an
18 opportunistic pathogen. *Nature*. 2000/09/13 ed. 2000;406: 959–964.
19 doi:10.1038/35023079
- 20 2. Hassett DJ, Korfhagen TR, Irvin RT, Schurr MJ, Sauer K, Lau GW, et al.
21 *Pseudomonas aeruginosa* biofilm infections in cystic fibrosis: insights into
22 pathogenic processes and treatment strategies. *Expert Opin Ther Targets*.
23 2010/01/09 ed. 2010;14: 117–130. doi:10.1517/14728220903454988

- 1 3. Livermore DM. Multiple mechanisms of antimicrobial resistance in
2 *Pseudomonas aeruginosa*: our worst nightmare? Clin Infect Dis. 2002;34: 634–
3 40. doi:10.1086/338782
- 4 4. Rodríguez-Rojas A, Oliver A, Blázquez J. Intrinsic and environmental mutagenesis
5 drive diversification and persistence of *Pseudomonas aeruginosa* in chronic lung
6 infections. J Infect Dis. 2012;205: 121–7. doi:10.1093/infdis/jir690
- 7 5. Oliver A, Canton R, Campo P, Baquero F, Blazquez J. High frequency of
8 hypermutable *Pseudomonas aeruginosa* in cystic fibrosis lung infection. Science
9 (80-). 2000/05/20 ed. 2000;288: 1251–1254. doi:8507 [pii]
- 10 6. Limoli DH, Rockel AB, Host KM, Jha A, Kopp BT, Hollis T, et al. Cationic
11 antimicrobial peptides promote microbial mutagenesis and pathoadaptation in
12 chronic infections. Ausubel FM, editor. PLoS Pathog. Public Library of Science;
13 2014;10: e1004083. doi:10.1371/journal.ppat.1004083
- 14 7. Rodríguez-Rojas A, Makarova O, Rolff J. Antimicrobials, stress and mutagenesis.
15 PLoS Pathog. 2014;10: e1004445. doi:10.1371/journal.ppat.1004445
- 16 8. Miller JH. Experiments in molecular genetics [Internet]. Cold Spring Harbor
17 Laboratory; 1972. Available:
18 [http://books.google.co.uk/books/about/Experiments_in_molecular_genetics.ht](http://books.google.co.uk/books/about/Experiments_in_molecular_genetics.html?id=PtVpAAAAMAAJ&pgis=1)
19 [ml?id=PtVpAAAAMAAJ&pgis=1](http://books.google.co.uk/books/about/Experiments_in_molecular_genetics.html?id=PtVpAAAAMAAJ&pgis=1)
- 20 9. Abdul-Tehrani H, Hudson AJ, Chang YS, Timms AR, Hawkins C, Williams JM, et al.
21 Ferritin mutants of *Escherichia coli* are iron deficient and growth impaired, and
22 fur mutants are iron deficient. J Bacteriol. 1999;181: 1415–28. Available:
23 [http://www.pubmedcentral.nih.gov/articlerender.fcgi?artid=93529&tool=pmce](http://www.pubmedcentral.nih.gov/articlerender.fcgi?artid=93529&tool=pmcentrez&rendertype=abstract)
24 [ntrez&rendertype=abstract](http://www.pubmedcentral.nih.gov/articlerender.fcgi?artid=93529&tool=pmcentrez&rendertype=abstract)
- 25 10. Yang Y, Harris DP, Luo F, Xiong W, Joachimiak M, Wu L, et al. Snapshot of iron
26 response in *Shewanella oneidensis* by gene network reconstruction. BMC
27 Genomics. 2009;10: 131. doi:10.1186/1471-2164-10-131

- 1 11. Girardello R, Bispo PJM, Yamanaka TM, Gales AC. Cation concentration
2 variability of four distinct Mueller-Hinton agar brands influences polymyxin B
3 susceptibility results. J Clin Microbiol. 2012;50: 2414–8. doi:10.1128/JCM.06686-
4 11
- 5 12. Imlay J, Chin S, Linn S. Toxic DNA damage by hydrogen peroxide through the
6 Fenton reaction in vivo and in vitro. Science (80-). 1988;240: 640–642.
7 doi:10.1126/science.2834821
- 8 13. Andrews SC, Robinson AK, Rodríguez-Quiriones F. Bacterial iron homeostasis.
9 FEMS Microbiol Rev. 2003;27: 215–37. Available:
10 <http://www.ncbi.nlm.nih.gov/pubmed/12829269>
- 11 14. Yamamoto Y, Fukui K, Koujin N, Ohya H, Kimura K, Kamio Y. Regulation of the
12 intracellular free iron pool by Dpr provides oxygen tolerance to Streptococcus
13 mutans. J Bacteriol. 2004;186: 5997–6002. doi:10.1128/JB.186.18.5997-
14 6002.2004
- 15 15. Reid DW, Carroll V, O'May C, Champion A, Kirov SM. Increased airway iron as a
16 potential factor in the persistence of Pseudomonas aeruginosa infection in cystic
17 fibrosis. Eur Respir J. 2007;30: 286–92. doi:10.1183/09031936.00154006
- 18 16. Reid DW, Carroll V, O'May C, Champion A, Kirov SM. Increased airway iron as a
19 potential factor in the persistence of Pseudomonas aeruginosa infection in cystic
20 fibrosis. Eur Respir J. 2007/05/17 ed. 2007;30: 286–292.
21 doi:09031936.00154006 [pii] 10.1183/09031936.00154006
- 22 17. Worlitzsch D, Tarran R, Ulrich M, Schwab U, Cekici A, Meyer KC, et al. Effects of
23 reduced mucus oxygen concentration in airway Pseudomonas infections of
24 cystic fibrosis patients. J Clin Invest. 2002/02/06 ed. 2002;109: 317–325.
25 doi:10.1172/JCI13870
- 26 18. Zasloff M. Antimicrobial peptides of multicellular organisms. Nature. 2002;415:
27 389–95. doi:10.1038/415389a

19. Ratledge C, Dover LG. Iron metabolism in pathogenic bacteria. *Annu Rev Microbiol. Annual Reviews* 4139 El Camino Way, P.O. Box 10139, Palo Alto, CA 94303-0139, USA; 2000;54: 881–941. doi:10.1146/annurev.micro.54.1.881
20. Nasnas R, Saliba G, Hallak P. [The revival of colistin: an old antibiotic for the 21st century]. *Pathol Biol.* 2008/01/08 ed. 2009;57: 229–235. doi:S0369-8114(07)00223-4 [pii] 10.1016/j.patbio.2007.09.013
21. Biswas S, Brunel J-M, Dubus J-C, Reynaud-Gaubert M, Rolain J-M. Colistin: an update on the antibiotic of the 21st century. *Expert Rev Anti Infect Ther.* 2012;10: 917–34. doi:10.1586/eri.12.78
22. Colistin: An Update on the Antibiotic of the 21st Century [Internet]. [cited 27 Aug 2015]. Available: http://www.medscape.com/viewarticle/772588_6
23. Hunter RC, Asfour F, Dingemans J, Osuna BL, Samad T, Malfroot A, et al. Ferrous iron is a significant component of bioavailable iron in cystic fibrosis airways. *MBio.* 2013;4: e00557–13–. doi:10.1128/mBio.00557-13
24. Kreamer NN, Costa F, Newman DK. The ferrous iron-responsive BqsRS two-component system activates genes that promote cationic stress tolerance. *MBio.* 2015;6: e02549. doi:10.1128/mBio.02549-14
25. Méhi O, Bogos B, Csörgő B, Pál F, Nyerges A, Papp B, et al. Perturbation of iron homeostasis promotes the evolution of antibiotic resistance. *Mol Biol Evol.* 2014;31: 2793–804. doi:10.1093/molbev/msu223
26. Wenzel M, Chiriac AI, Otto A, Zweytick D, May C, Schumacher C, et al. Small cationic antimicrobial peptides delocalize peripheral membrane proteins. *Proc Natl Acad Sci U S A.* 2014;111: E1409–18. doi:10.1073/pnas.1319900111
27. Goldman MJ, Anderson GM, Stolzenberg ED, Kari UP, Zasloff M, Wilson JM. Human beta-defensin-1 is a salt-sensitive antibiotic in lung that is inactivated in cystic fibrosis. *Cell.* 1997;88: 553–60. Available: <http://www.ncbi.nlm.nih.gov/pubmed/9038346>

- 1 28. McPhee JB, Bains M, Winsor G, Lewenza S, Kwasnicka A, Brazas MD, et al.
2 Contribution of the PhoP-PhoQ and PmrA-PmrB two-component regulatory
3 systems to Mg²⁺-induced gene regulation in *Pseudomonas aeruginosa*. J
4 Bacteriol. 2006/05/19 ed. 2006;188: 3995–4006. doi:188/11/3995 [pii]
5 10.1128/JB.00053-06
- 6 29. Moskowitz SM, Ernst RK, Miller SI. PmrAB, a two-component regulatory system
7 of *Pseudomonas aeruginosa* that modulates resistance to cationic antimicrobial
8 peptides and addition of aminoarabinose to lipid A. J Bacteriol. 2004;186: 575–
9 9. Available:
10 <http://www.pubmedcentral.nih.gov/articlerender.fcgi?artid=305751&tool=pmc>
11 [entrez&rendertype=abstract](http://www.pubmedcentral.nih.gov/articlerender.fcgi?artid=305751&tool=pmc)
- 12 30. Marlovits TC, Haase W, Herrmann C, Aller SG, Unger VM. The membrane protein
13 FeoB contains an intramolecular G protein essential for Fe(II) uptake in bacteria.
14 Proc Natl Acad Sci U S A. 2002;99: 16243–8. doi:10.1073/pnas.242338299
- 15 31. Oliver A. High Frequency of Hypermutable *Pseudomonas aeruginosa* in Cystic
16 Fibrosis Lung Infection. Science (80-). 2000;288: 1251–1253.
17 doi:10.1126/science.288.5469.1251
- 18 32. Couce A, Rodríguez-Rojas A, Blázquez J. Bypass of genetic constraints during
19 mutator evolution to antibiotic resistance. Proc Biol Sci. 2015;282: 20142698.
20 doi:10.1098/rspb.2014.2698
- 21 33. Imlay J a. Cellular defenses against superoxide and hydrogen peroxide. Annu Rev
22 Biochem. 2008;77: 755–76. doi:10.1146/annurev.biochem.77.061606.161055
- 23 34. Rodríguez-Rojas A, Couce A, Blázquez J. Frequency of spontaneous resistance to
24 fosfomycin combined with different antibiotics in *Pseudomonas aeruginosa*.
25 Antimicrob Agents Chemother. 2010/08/18 ed. 2010;54: 4948–4949.
26 doi:AAC.00415-10 [pii] 10.1128/AAC.00415-10
- 27 35. Rodríguez-Rojas A, Maciá MD, Couce A, Gómez C, Castañeda-García A, Oliver A,
28 et al. Assessing the Emergence of Resistance: the Absence of Biological Cost in

- 1 vivo May Compromise Fosfomycin Treatments for *P. aeruginosa* Infections. PLoS
2 One. 2010;(In press).
- 3 36. Castaneda-Garcia A, Rodriguez-Rojas A, Guelfo JR, Blazquez J. The Glycerol-3-
4 Phosphate Permease GlpT Is the Only Fosfomycin Transporter in *Pseudomonas*
5 *aeruginosa*. J Bacteriol. 2009/09/08 ed. 2009;191: 6968–6974. doi:JB.00748-09
6 [pii] 10.1128/JB.00748-09
- 7 37. Rodriguez-Rojas A, Blazquez J. The *Pseudomonas aeruginosa* pfpl gene plays an
8 antimutator role and provides general stress protection. J Bacteriol. 2008/11/26
9 ed. 2009;191: 844–850. doi:JB.01081-08 [pii] 10.1128/JB.01081-08
- 10 38. Rodríguez-Rojas A, Maciá MD, Couce A, Gómez C, Castañeda-García A, Oliver A,
11 et al. Assessing the emergence of resistance: the absence of biological cost in
12 vivo may compromise fosfomycin treatments for *P. aeruginosa* infections. PLoS
13 One. 2010;5: e10193. doi:10.1371/journal.pone.0010193
- 14 39. Morgan C, Lewis PD. iMARS - Mutation analysis reporting software: An analysis
15 of spontaneous cII mutation spectra. Mutat Res - Genet Toxicol Environ
16 Mutagen. 2006;603: 15–26. doi:10.1016/j.mrgentox.2005.09.010
- 17 40. McBride TJ, Preston BD, Loeb LA. Mutagenic spectrum resulting from DNA
18 damage by oxygen radicals. Biochemistry. 1991;30: 207–13. Available:
19 <http://www.ncbi.nlm.nih.gov/pubmed/1703014>
- 20 41. Juurik T, Ilves H, Teras R, Ilmjärv T, Tavita K, Ukkivi K, et al. Mutation frequency
21 and spectrum of mutations vary at different chromosomal positions of
22 *Pseudomonas putida*. PLoS One. 2012;7: e48511.
23 doi:10.1371/journal.pone.0048511
- 24 42. Shee C, Gibson JL, Rosenberg SM. Two mechanisms produce mutation hotspots
25 at DNA breaks in *Escherichia coli*. Cell Rep. 2012;2: 714–21.
26 doi:10.1016/j.celrep.2012.08.033

- 1 43. Moyano AJ, Luján AM, Argaraña CE, Smania AM. MutS deficiency and activity of
2 the error-prone DNA polymerase IV are crucial for determining mucA as the
3 main target for mucoid conversion in *Pseudomonas aeruginosa*. *Mol Microbiol.*
4 2007;64: 547–59. doi:10.1111/j.1365-2958.2007.05675.x
- 5 44. Lofton H, Pránting M, Thulin E, Andersson DI. Mechanisms and fitness costs of
6 resistance to antimicrobial peptides LL-37, CNY100HL and wheat germ histones.
7 *PLoS One*. 2013;8: e68875. doi:10.1371/journal.pone.0068875
- 8 45. Foti JJ, Devadoss B, Winkler JA, Collins JJ, Walker GC. Oxidation of the guanine
9 nucleotide pool underlies cell death by bactericidal antibiotics. *Science*.
10 2012;336: 315–9. doi:10.1126/science.1219192
- 11 46. Kohanski M a, DePristo M a, Collins JJ. Sublethal antibiotic treatment leads to
12 multidrug resistance via radical-induced mutagenesis. *Mol Cell*. Elsevier Ltd;
13 2010;37: 311–20. doi:10.1016/j.molcel.2010.01.003
- 14 47. Kohanski MA, Dwyer DJ, Hayete B, Lawrence CA, Collins JJ. A common
15 mechanism of cellular death induced by bactericidal antibiotics. *Cell*.
16 2007/09/07 ed. 2007;130: 797–810. doi:S0092-8674(07)00899-9 [pii]
17 10.1016/j.cell.2007.06.049
- 18 48. Dwyer DJ, Kohanski MA, Collins JJ. Role of reactive oxygen species in antibiotic
19 action and resistance. *Curr Opin Microbiol*. 2009/08/04 ed. 2009;12: 482–489.
20 doi:S1369-5274(09)00090-3 [pii] 10.1016/j.mib.2009.06.018
- 21 49. Keren I, Wu Y, Inocencio J, Mulcahy LR, Lewis K. Killing by bactericidal antibiotics
22 does not depend on reactive oxygen species. *Science*. 2013;339: 1213–6.
23 doi:10.1126/science.1232688
- 24 50. Liu Y, Imlay J a. Cell Death from Antibiotics Without the Involvement of Reactive
25 Oxygen Species. *Science (80-)*. 2013;339: 1210–1213.
26 doi:10.1126/science.1232751

- 1 51. Imlay JA. Diagnosing oxidative stress in bacteria: not as easy as you might think.
2 Curr Opin Microbiol. 2015;24C: 124–131. doi:10.1016/j.mib.2015.01.004
- 3 52. Ward CG, Bullen JJ, Rogers HJ. Iron and infection: new developments and their
4 implications. J Trauma. 1996/08/01 ed. 1996;41: 356–364. Available:
5 [http://www.ncbi.nlm.nih.gov/entrez/query.fcgi?cmd=Retrieve&db=PubMed&d](http://www.ncbi.nlm.nih.gov/entrez/query.fcgi?cmd=Retrieve&db=PubMed&dopt=Citation&list_uids=8760553)
6 [opt=Citation&list_uids=8760553](http://www.ncbi.nlm.nih.gov/entrez/query.fcgi?cmd=Retrieve&db=PubMed&dopt=Citation&list_uids=8760553)
- 7 53. Wessling-Resnick M. Iron homeostasis and the inflammatory response. Annu
8 Rev Nutr. 2010;30: 105–22. doi:10.1146/annurev.nutr.012809.104804
- 9 54. Skaar EP. The battle for iron between bacterial pathogens and their vertebrate
10 hosts. PLoS Pathog. 2010;6: e1000949. doi:10.1371/journal.ppat.1000949
- 11 55. Couce A, Blazquez J. Estimating mutation rates in low-replication experiments.
12 Mutat Res. 2011/07/09 ed. 2011;In Press. doi:S0027-5107(11)00147-3 [pii]
13 10.1016/j.mrfmmm.2011.06.005
- 14 56. Hall BM, Ma C-X, Liang P, Singh KK. Fluctuation analysis CalculatOR: a web tool
15 for the determination of mutation rate using Luria-Delbruck fluctuation analysis.
16 Bioinformatics. 2009;25: 1564–5. doi:10.1093/bioinformatics/btp253
- 17 57. West SE, Schweizer HP, Dall C, Sample AK, Runyen-Janecky LJ. Construction of
18 improved Escherichia-Pseudomonas shuttle vectors derived from pUC18/19 and
19 sequence of the region required for their replication in Pseudomonas
20 aeruginosa. Gene. 1994/10/11 ed. 1994;148: 81–86. doi:0378-1119(94)90237-2
21 [pii]
- 22 58. Vilchèze C, Hartman T, Weinrick B, Jacobs WR. Mycobacterium tuberculosis is
23 extraordinarily sensitive to killing by a vitamin C-induced Fenton reaction. Nat
24 Commun. Nature Publishing Group, a division of Macmillan Publishers Limited.
25 All Rights Reserved.; 2013;4: 1881. doi:10.1038/ncomms2898

59. Riemer J, Hoepken HH, Czerwinska H, Robinson SR, Dringen R. Colorimetric
ferrozine-based assay for the quantitation of iron in cultured cells. Anal
Biochem. 2004;331: 370–5. doi:10.1016/j.ab.2004.03.049

Supplement figure and table legends

Figure S1. Different concentrations of LL-37 (from 4 to 32 µg/ml) have no impact on
mutant frequencies to rifampicin of *P. aeruginosa* PAO1 in MHB. Error bars represent
95 % confidence intervals for mutant frequencies.

Figure S2. Different concentrations of Fe²⁺ have no impact on mutant frequencies to
rifampicin of *P. aeruginosa* PAO1. Error bars represent 95 % confidence intervals for
mutant frequencies.

Figure S3. Different concentrations of Fe²⁺ increase mutant frequencies to rifampicin
of *P. aeruginosa* PAO1 if LL-37 is present. The experiment was carried out at MIC50 for
LL-37 (32 µg/ml). Error bars represent 95 % confidence intervals for mutant
frequencies.

Figure S4. The combination of Fe²⁺ (40 µM) and LL-37 (32 µg/ml) increases the mutant
frequency of *P. aeruginosa* PA14 to fosfomycin. Error bars represent 95 % confidence
intervals for mutant frequencies.

Figure S5. 3D-structural model of GlpT. A homology model of GlpT was generated
using Cn3D software by performing a BLASTP search using PA14 GlpT protein sequence
as a query and mapping the resulting alignment against the experimentally determined
Escherichia coli K-12 GlpT protein structure. Substitutions found in Fos-R mutants in all
treatments are highlighted in yellow.

1

2 **Figure S6.** DNA alignment of the 1160 bp fragment of *glpT* from twenty Fos-R *P.*
3 *aeruginosa* PA14 clones treated with iron, LL-37 and LL-37+Fe²⁺. The 52-1212 bp region
4 relative to the A in the start ATG codon of the 1347bp-long *glpT* ORF.

5

6 **Figure S7.** Mutation types in *glpT*. Prevalence of certain mutation types in iron, LL-37
7 and LL-37+Fe²⁺ treatments. C to T transitions was the most common type of nucleotide
8 substitutions in LL-37+Fe²⁺ treatment, but not in two other treatments.

9 **Table S1.** Mutations in *glpT* of Fos-R *P. aeruginosa* PA14 clones treated with iron, LL-37
10 and LL-37+Fe²⁺.

11

12 **Table S2.** Two-tailed Fisher's exact-test of probability of having the same mutation in
13 both LL-37 and iron treatments. H0 is rejected if $P < 0.05$.

14

15 **Table S3.** Two-tailed Fisher's exact-test of probability of having the same mutation in
16 both LL-37 and LL-37+Fe²⁺ treatments. H0 is rejected if $P < 0.05$. Mutation hotspots that
17 significantly different are highlighted.

18

19

20 **Table S4.** Two-tailed Fisher's exact-test of probability of having the same mutation in
21 both iron and LL-37+Fe²⁺ treatments. H0 is rejected if $P < 0.05$. Mutation hotspots that
22 significantly different are highlighted.

23

24

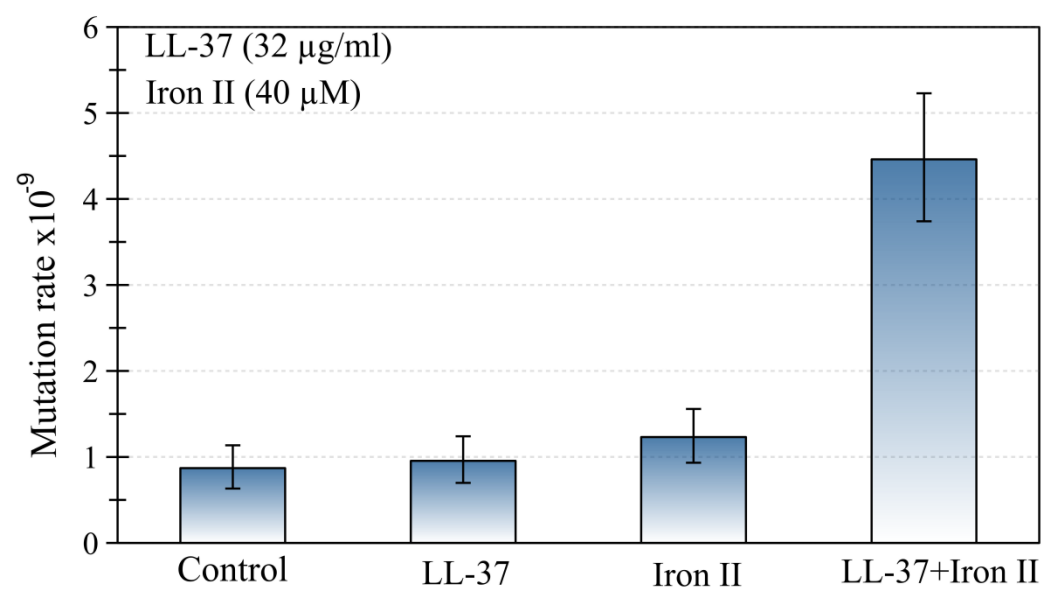


Figure 1.

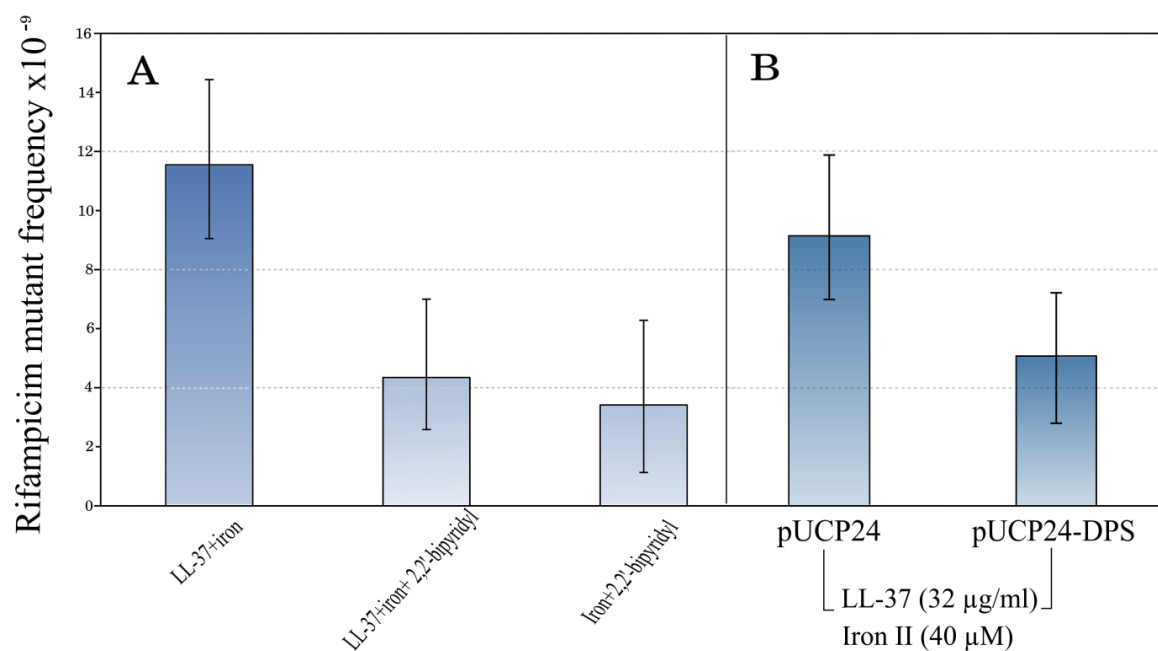


Figure 2.

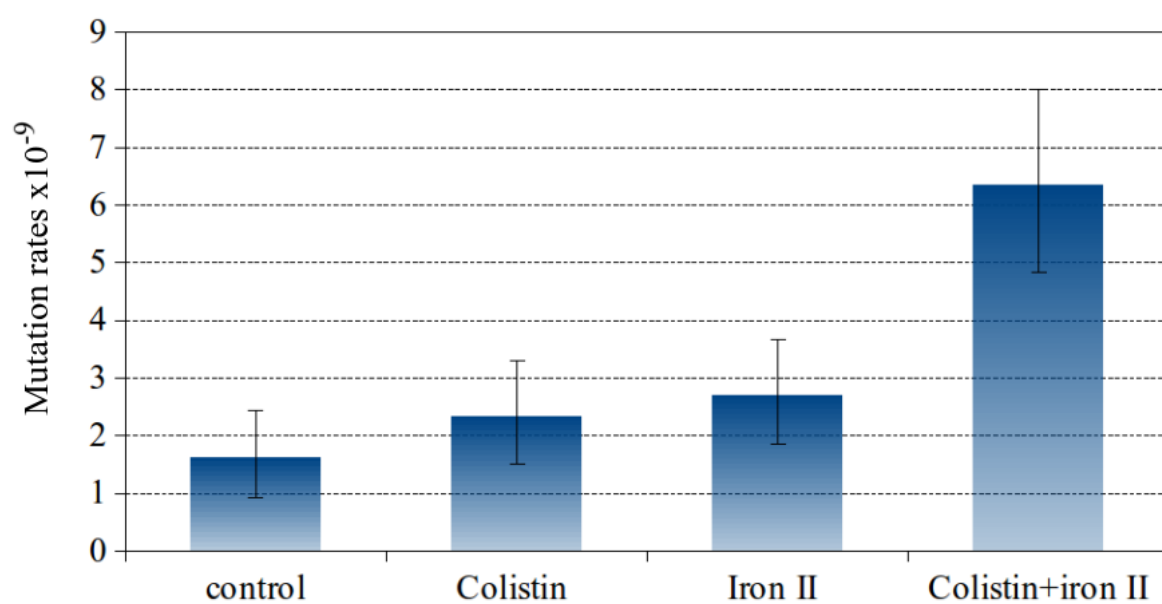


Figure 3.

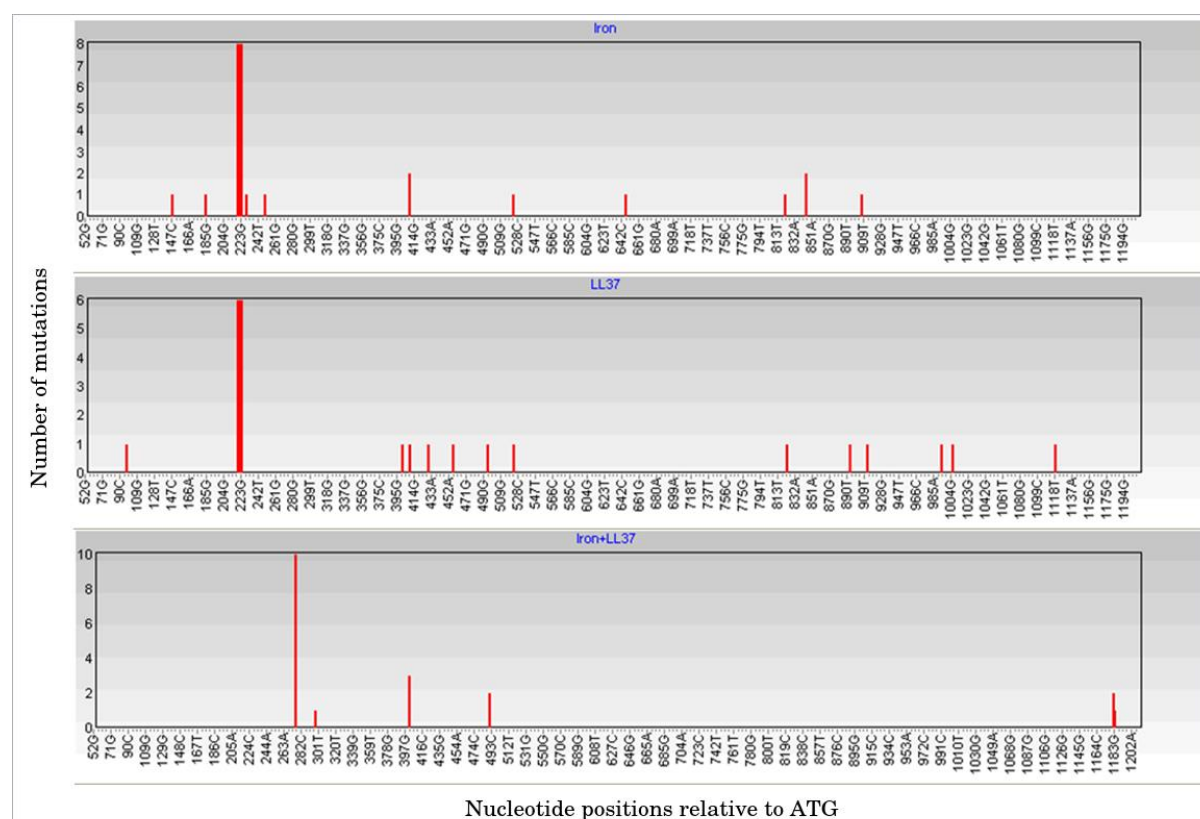


Figure 4.

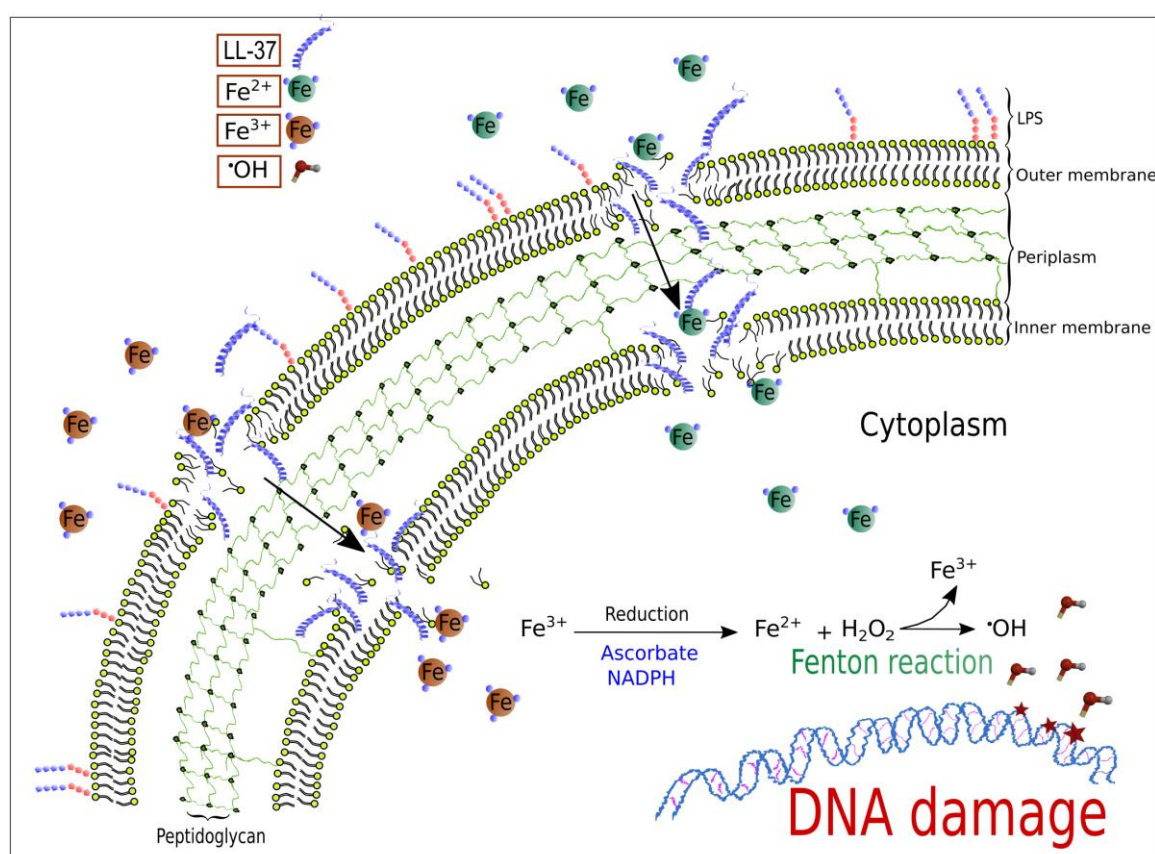


Figure 5.

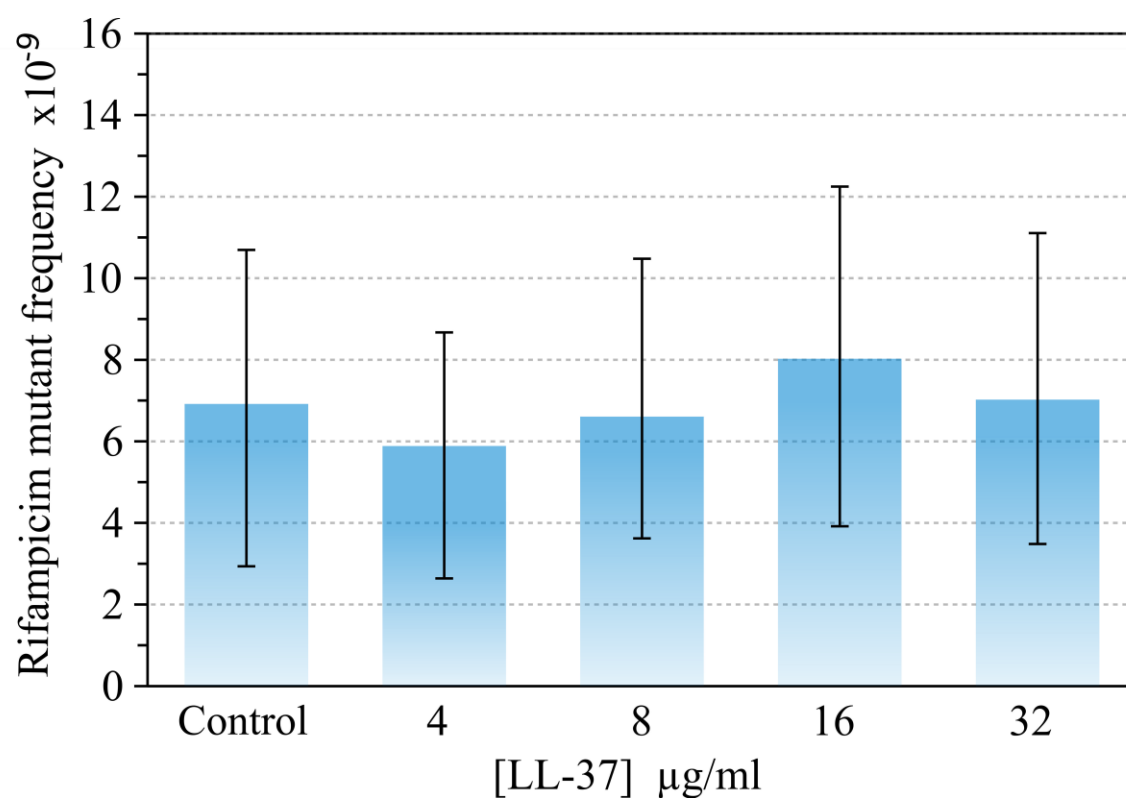


Figure S1.

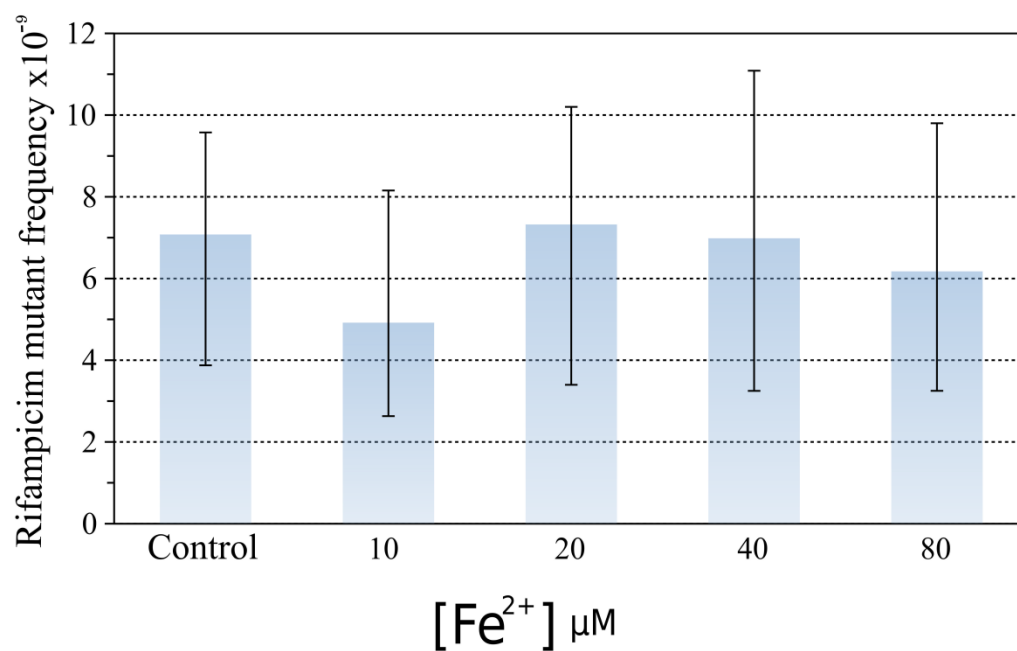


Figure S2.

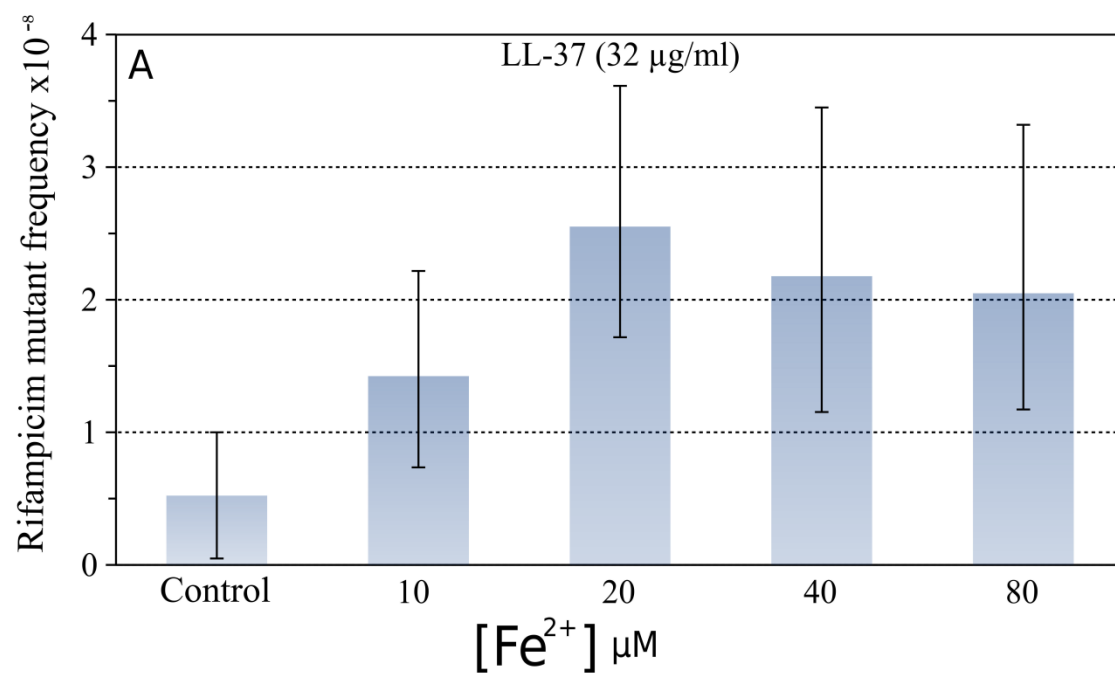


Figure S3.

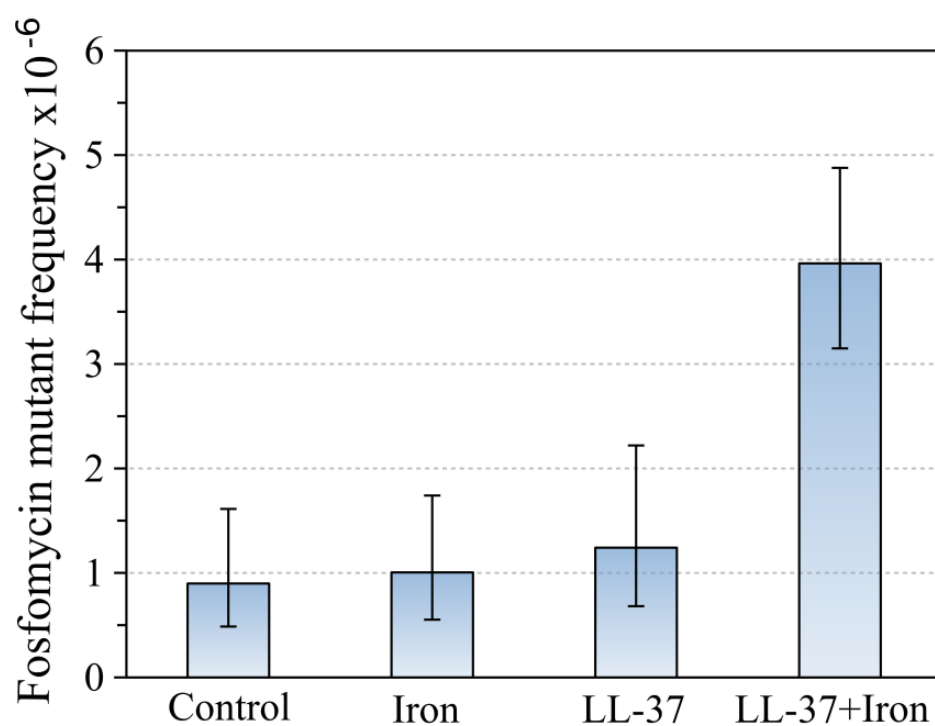


Figure S4.

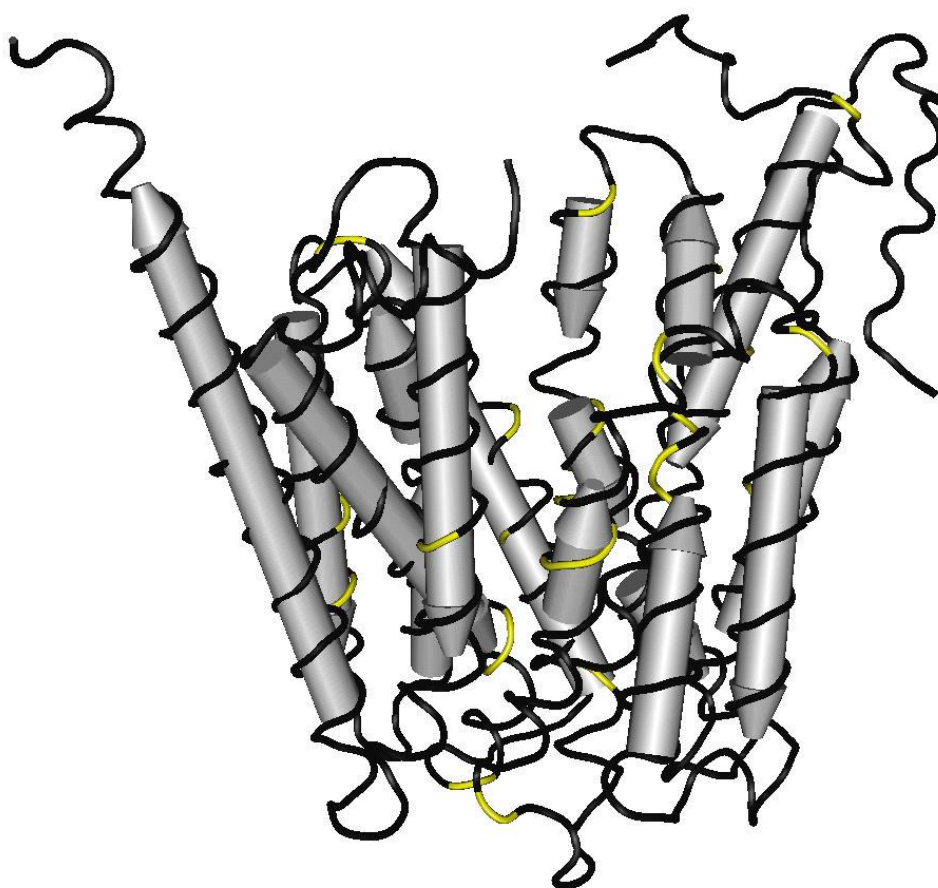


Figure S5.

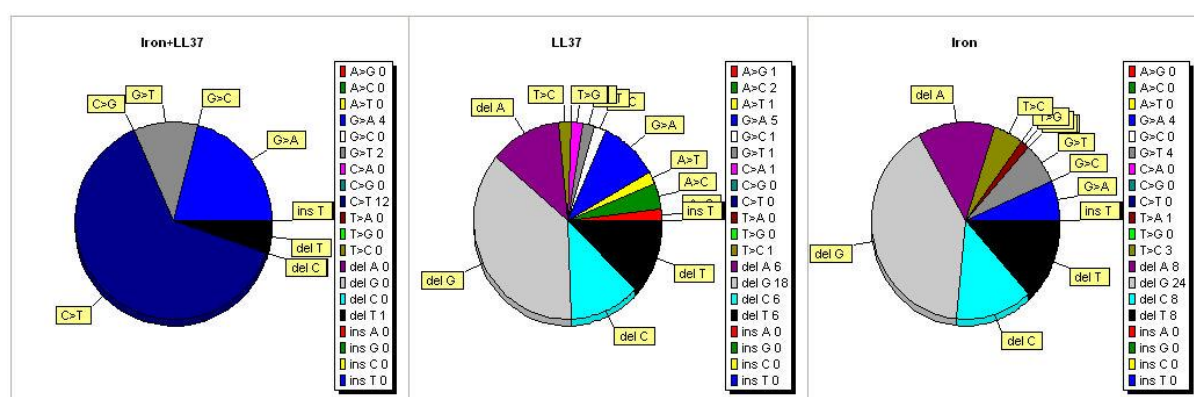


Figure S7.

Table S1. Mutations in *glpT* of Fos-R *P. aeruginosa* PA14 clones treated with iron, LL-37 and LL-37+Fe²⁺

Treatment	Mutant number	Mutation position ¹	Amino acid change ²	Protein stability ddG Value ³	Protein domain ⁴
Iron	1	G230 to A transition	G77 to D	-1.09 Large Decrease of Stability	TMhelix
	2	A220TCGCC225, deletion 6 bp	deletion of I74- A75	NA	TMhelix
	3	A846 to T transversion	E282 to V	0.08 Increase of Stability	outside
	4	G185 to A transition	R62 to H	-1.33 Large Decrease of Stability	outside
	5	A846 to T transversion	E282 to V	0.08 Increase of Stability	outside
	6	G250 to T transversion	G84 to C	-1.38Large Decrease of Stability	TMhelix
	7	G409 to A	G137 to S	-1.01 Large Decrease of Stability	TMhelix
	8	T908 to C transition	I303 to T	-2.05 Large Decrease of Stability	TMhelix
	9	T823 to A transversion	W275 to R	-1.09 Large Decrease of Stability	outside
	10	A220TCGCC225, deletion 6 bp	deletion of I74- A75	NA	TMhelix
	11	A220TCGCC225, deletion 6 bp	deletion of I74- A75	NA	TMhelix
	12	T149 to C transition	L50 to P	-1.91 Large Decrease of Stability	outside
	13	A220TCGCC225, deletion 6 bp	deletion of I74- A75	NA	TMhelix
	14	A220TCGCC225, deletion 6 bp	deletion of I74- A75	NA	TMhelix
	15	A220TCGCC225, deletion 6 bp	deletion of I74- A75	NA	TMhelix
	16	A220TCGCC225, deletion 6 bp	deletion of I74- A75	NA	TMhelix
	17	A220TCGCC225, deletion 6 bp	deletion of I74- A75	NA	TMhelix
	18	G409 to T	G137 to C	-0.84 Large Decrease of Stability	TMhelix
	19	T524 to C transition	L175 to P	-1.06 Large Decrease of Stability	TMhelix
	20	G647 to A transition	G216 to D	-1.03 Large Decrease of Stability	inside
LL-37	1	A496 to G transition	N166 to D	-0.08 Decrease of Stability	TMhelix
	2	A220TCGCC225, deletion 6 bp	deletion of I74- A75	NA	TMhelix
	3	A1006 to C transversion	T336 to P	-0.70 Large Decrease of Stability	TMhelix
	4	A401 to T transversion	Q134 to L	-0.10 Decrease of Stability	TMhelix
	5	A220TCGCC225, deletion 6 bp	deletion of I74- A75	NA	TMhelix
	6	T524 to C transition	L175 to P	-1.06 Large Decrease of Stability	TMhelix
	7	A220TCGCC225, deletion 6 bp	deletion of I74- A75	NA	TMhelix
	8	C894 to A transversion, stop codon	Y298 to stop , truncation	NA	NA
	9	A220TCGCC225, deletion 6 bp	deletion of I74- A75	NA	TMhelix

LL-37+Fe ²⁺	10	G98 to A transition	G33 to D	-0.95, Large Decrease of Stability	TMhelix
	11	A220TCGCC225, deletion 6 bp	deletion of I74- A75	NA	TMhelix
	12	G994 to C transversion	V332 to L	-1.30 Large Decrease of Stability	TMhelix
	13	G457 to A transition	E153 to K	-0.70 Large Decrease of Stability	inside
	14	G409 to T	G137 to C	-0.84 Large Decrease of Stability	TMhelix
	15	A430 to C transversion	T144 to P	-0.39 Decrease of Stability	inside
	16	G1120 to A transition	E374 to K	-0.49 Decrease of Stability	Inside
	17	G824 to A transition, stop codon	W275 to stop , truncation	NA	outside
	18	A220TCGCC225, deletion 6 bp	deletion of I74- A75	NA	TMhelix
	19	G913 to A transition	G305 to S	-1.10 Large Decrease of Stability	TMhelix
	20	G229 to A transition	G77 to S	-1.23 Large Decrease of Stability	TMhelix
	1	G403 to A transition	G135 to S	-1.05 Large Decrease of Stability	TMhelix
	2	C277 to T transition	R93 to W	-0.57 Large Decrease of Stability	inside
	2	G403 to T transversion	G135 to C	-0.90 Large Decrease of Stability	TMhelix
	3	C822 to G transversion	D274 to E	-0.08 Decrease of Stability	outside
	4	C277 to T transition	R93 to W	-0.57 Large Decrease of Stability	inside
	5	C277 to T transition	R93 to W	-0.57 Large Decrease of Stability	inside
	6	G1183 to A transition	G395 to S	-1.20 Large Decrease of Stability	TMhelix
	7	C277 to T transition	R93 to W	-0.57 Large Decrease of Stability	inside
	8	C277 to T transition	R93 to W	-0.57 Large Decrease of Stability	inside
	9	C277 to T transition	R93 to W	-0.57 Large Decrease of Stability	inside
	10	G1184 to A transition	G395 to D	-0.85 Large Decrease of Stability	TMhelix
	11	C491 to T transition	A164 to V	0.01 Increase of Stability	TMhelix
	12	C491 to T transition	A164 to V	0.01 Increase of Stability	TMhelix
	13	C822 to G transversion	D274 to E	-0.08 Decrease of Stability	outside
	14	C277 to T transition	R93 to W	-0.57 Large Decrease of Stability	inside
	15	C277 to T transition	R93 to W	-0.57 Large Decrease of Stability	inside
	16	C277 to T transition	R93 to W	-0.57 Large Decrease of Stability	inside
	17	C277 to T transition	R93 to W	-0.57 Large Decrease of Stability	inside
	18	T299, deletion 1bp, frameshift	frameshift	NA	NA

19	G1183 to A transition	G395 to S	-1.20 Large Decrease of Stability	TMhelix
20	G403 to T transition	G135 to C	-0.90 Large Decrease of Stability	TMhelix

¹ relative to the A in the start ATG codon of the 1347bp-long *glpT* ORF

² relative to the first amino acid of the GlpT protein

³ ddG values are calculated using I-Mutant3.0 software for prediction of the protein stability change upon mutation, available from http://gpcr.biocomp.unibo.it/~emidio/I-Mutant3.0/I-MutantDDG_Help.html

⁴ location of transmembrane helices in proteins was predicted using TMHMM Server v. 2.0, available from <http://www.cbs.dtu.dk/services/TMHMM-2.0/>

Table S2.

Mutation site	Number of mutants per treatment		Two-tailed <i>P</i> -value	Interpretation
	LL-37	Iron		
G33 to D	1	0	> 0.9999	The groups are not significantly different.
L50 to P	0	1	> 0.9999	The groups are not significantly different.
R62 to H	0	1	> 0.9999	The groups are not significantly different.
deletion of 6 bp I74 - A75	6	8	0.7411	The groups are not significantly different.
G77 to D	1	1	> 0.9999	The groups are not significantly different.
G84 to C	0	1	> 0.9999	The groups are not significantly different.
R93 to W	0	0	> 0.9999	The groups are not significantly different.
Q134 to L	1	0	> 0.9999	The groups are not significantly different.
G135 to S	0	0	> 0.9999	The groups are not significantly different.
G137 to S	1	2	> 0.9999	The groups are not significantly different.
T299 frameshift	0	0	> 0.9999	The groups are not significantly different.
T144 to P	1	0	> 0.9999	The groups are not significantly different.
E153 to K	1	0	> 0.9999	The groups are not significantly different.
N166 to D	1	0	> 0.9999	The groups are not significantly different.
A164 to V	0	0	> 0.9999	The groups are not significantly different.
L175 to P	1	1	> 0.9999	The groups are not significantly different.
G216 to D	0	1	> 0.9999	The groups are not significantly different.
D274 to E	0	0	> 0.9999	The groups are not significantly different.
W275 to R	1	1	> 0.9999	The groups are not significantly different.
E282 to V	0	2	0.4872	The groups are not significantly different.
Y298 to stop, truncation	1	0	> 0.9999	The groups are not significantly different.
I303 to T	0	1	> 0.9999	The groups are not significantly different.
G305 to S	1	0	> 0.9999	The groups are not significantly different.
V332 to L	1	0	> 0.9999	The groups are not significantly different.
T336 to P	1	0	> 0.9999	The groups are not significantly different.
E374 to K	1	0	> 0.9999	The groups are not significantly different.
G395 to S	0	0	> 0.9999	The groups are not significantly different.

Table S3.

Mutation site	Number of mutants per treatment		Two-tailed <i>P</i> -value	Interpretation
	LL-37	LL-37+Fe ²⁺		
G33 to D	1	0	> 0.9999	The groups are not significantly different.
L50 to P	0	0	> 0.9999	The groups are not significantly different.
R62 to H	0	0	> 0.9999	The groups are not significantly different.
deletion of 6 bp I74 - A75	6	0	0.0202	The groups are significantly different.
G77 to D	1	0	> 0.9999	The groups are not significantly different.
G84 to C	0	0	> 0.9999	The groups are not significantly different.
R93 to W	0	10	0.0004	The groups are significantly different.
Q134 to L	1	0	> 0.9999	The groups are not significantly different.
G135 to S	0	3	0.2308	The groups are not significantly different.
G137 to S	1	0	> 0.9999	The groups are not significantly different.
T299 frameshift	0	1	> 0.9999	The groups are not significantly different.
T144 to P	1	0	> 0.9999	The groups are not significantly different.
E153 to K	1	0	> 0.9999	The groups are not significantly different.
N166 to D	1	0	> 0.9999	The groups are not significantly different.
A164 to V	0	2	0.4872	The groups are not significantly different.
L175 to P	1	0	> 0.9999	The groups are not significantly different.
G216 to D	0	0	> 0.9999	The groups are not significantly different.
D274 to E	0	2	0.4872	The groups are not significantly different.
W275 to R	1	0	> 0.9999	The groups are not significantly different.
E282 to V	0	0	> 0.9999	The groups are not significantly different.
Y298 to stop, truncation	1	0	> 0.9999	The groups are not significantly different.
I303 to T	0	0	> 0.9999	The groups are not significantly different.
G305 to S	1	0	> 0.9999	The groups are not significantly different.
V332 to L	1	0	> 0.9999	The groups are not significantly different.
T336 to P	1	0	> 0.9999	The groups are not significantly different.
E374 to K	1	0	> 0.9999	The groups are not significantly different.
G395 to S	0	3	0.2308	The groups are not significantly different.

Table S4.

Mutation site	Number of mutants per treatment		Two-tailed <i>P</i> -value	Interpretation
	Iron	LL-37+Fe ²⁺		
G33 to D	0	0	> 0.9999	The groups are not significantly different.
L50 to P	1	0	> 0.9999	The groups are not significantly different.
R62 to H	1	0	> 0.9999	The groups are not significantly different.
deletion of 6 bp I74 - A75	8	0	0.0033	The groups are significantly different.
G77 to D	1	0	> 0.9999	The groups are not significantly different.
G84 to C	1	0	> 0.9999	The groups are not significantly different.
R93 to W	0	10	0.0004	The groups are significantly different.
Q134 to L	0	0	> 0.9999	The groups are not significantly different.
G135 to S	0	3	0.2308	The groups are not significantly different.
G137 to S	2	0	0.4872	The groups are not significantly different.
T299 frameshift	0	1	> 0.9999	The groups are not significantly different.
T144 to P	0	0	> 0.9999	The groups are not significantly different.
E153 to K	0	0	> 0.9999	The groups are not significantly different.
N166 to D	0	0	> 0.9999	The groups are not significantly different.
A164 to V	0	2	0.4872	The groups are not significantly different.
L175 to P	1	0	> 0.9999	The groups are not significantly different.
G216 to D	1	0	> 0.9999	The groups are not significantly different.
D274 to E	0	2	0.4872	The groups are not significantly different.
W275 to R	1	0	> 0.9999	The groups are not significantly different.
E282 to V	2	0	> 0.9999	The groups are not significantly different.
Y298 to stop, truncation	0	0	> 0.9999	The groups are not significantly different.
I303 to T	1	0	> 0.9999	The groups are not significantly different.
G305 to S	0	0	> 0.9999	The groups are not significantly different.
V332 to L	0	0	> 0.9999	The groups are not significantly different.
T336 to P	0	0	> 0.9999	The groups are not significantly different.
E374 to K	0	0	> 0.9999	The groups are not significantly different.
G395 to S	0	3	0.2308	The groups are not significantly different.

LL37Iron_18	90
LL37Iron_19	90
LL37Iron_20	90

[illegible]

LL37Iron_18	180
LL37Iron_19	180
LL37Iron_20	180

[illegible]

LL37Iron_18 269
LL37Iron_19 270
LL37Iron_20 270

[illegible]

LL37Iron_18	359
LL37Iron_19	360
LL37Iron_20 T	360

9

LL37Iron_18 449
LL37Iron_19 450
LL37Iron_20 450

[illegible]

LL37Iron_18 539
LL37Iron_19 540
LL37Iron_20 540

13

LL37Iron_18 629
LL37Iron_19 630
LL37Iron_20 630

[illegible]

LL37Iron_18	719
LL37Iron_19	720
LL37Iron_20	720

[illegible]

LL37Iron_18	809
LL37Iron_19	810
LL37Iron_20	810

19

LL37Iron_18	899
LL37Iron_19	900
LL37Iron_20	900

21

LL37Iron_18 989
LL37Iron_19 990
LL37Iron_20 990

[illegible]

LL37Iron_18	...	1079
LL37Iron_19	...	1080
LL37Iron_20	...	1080

25

